Modeling of the control system to optimize the displacement of an omnidirectional single-seater with Mecanum wheels.

Caiza Chiguano, Luis David y Peña Obaco, Ronny Antonio

Departamento de Energía y Mecánica

Carrera de Ingeniería Automotriz

Artículo académico, previo a la obtención del título de Ingeniero Automotriz

Ing. Terán Herrera, Héctor Cochise e Ing. Zambrano León, Víctor Danilo

23 de Agosto del 2021

978-1-7281-5281-3/20/$31.00@2020 IEEE

Modeling of the control system to optimize the displacement of an omnidirectional single-seater with Mecanum wheels.

Luis D. Caiza, Ronny A. Peña, Héctor C. Terán and Víctor D. Zambrano
Departamento de Ciencias de la Energía y Mecánica
Universidad de las Fuerzas Armadas ESPE
Sangolquí, Ecuador
ldcaiza1@espe.edu.ec, rapena1@espe.edu.ec, hcteran@espe.edu.ec, vdzambrano@espe.edu.ec

***Abstract*—. The study proposes the optimization of an omnidirectional single-seater with Mecanum wheels with respect to their displacement, through the implementation of an adaptive electronic control system. The torque and speed required for the displacement are defined by the weight, center of mass and radius of the wheel. The control elements, data processing and user interaction were implemented to work in sync with a brushless motor (BLDC). The communication between components was done through the control algorithm developed on the Arduino platform. This microcontroller interprets voltage signals generated by a Joystick, processes them with the kinematic model and sets the rotation speed in each wheel, through the pulse width variation (PWM). To validate it, displacement tests were carried out on two types of surfaces: asphalt and concrete, with trajectory deviations at different speeds. Consequently, a mathematical model with correction factor was determined. This model fed back to the control algorithm, showing optimized stabilization, displacement and trajectory tracking of the single-seater.**

Keywords-component; single-seater, optimization, Mecanum wheel, surfaces, omnidirectional movement.

I. INTRODUCTION

The development of modern cities has increased the demand for transportation [1,2], resulting in high vehicular flow, congestion, frequent accidents, and shortage of parking spaces [3,4]. Conventional vehicles make turns with the Ackerman steering mechanism, which acts on the front wheels, orienting them in a sharp range, this prevents direct positioning of the vehicle, which requires more space and steering control to move [5,6].

Omnidirectional locomotion can be performed in any direction, without the need to position oneself before starting to move [7]. This movement is produced through the control of special wheels called Mecanum [8], whose design is a central wheel provided with rollers around its periphery. The rollers are positioned at an angle of 45º to the center axis of the wheel [9]. The optimized control software and under normal conditions, allows the vehicle to move at average speeds. This is achieved with a kinematic model [10], which validates the omnidirectional motion configured for Mecanum wheels.

The improved movements achieved with the implemented system are a sustainable mobility alternative for the population seeking compact, personal and less polluting vehicles [11]. For the study, a single-seater with omnidirectional traction was designed, built and validated. Different displacement tests were carried out on different surfaces with all possible movements for this type of vehicle. For the study, a single-seater with omnidirectional traction was designed, built and validated, running displacement tests on different surfaces and performing all possible movements for this type of vehicle.

By varying the surface conditions, the objective is to obtain an adequate optimization of the single-seater to improve mobility and maneuverability in dynamic and limited spaces [8].

II. OMNIDIRECTIONAL DESIGN

In Fig.1 the omnidirectional control works with electronic (a) and mechanical (b) components. The microcontroller (MCU) receives signals sent by the joystick, these are processed and vary the pulse width (PWM) required by the speed controller (ESC). This allows the operation of the brushless motor (BLDC) coupled to a planetary gearbox (CIM), increasing the torque that activates the Mecanum wheel.

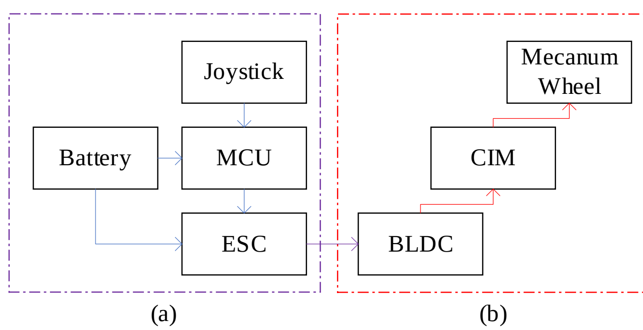

Figure 1: Omni-directional control, (a) Electronic components, (b) Mechanical components

III. CONTROL SCHEME

The omnidirectional control system is designed to adapt to different types of surfaces and consists of three phases of operation: the displacement phase with the Mecanum wheels, automation via MCU and optimization of the control signals received by the ESCs.

These phases communicate with each other, Fig. 2, in order to modify the motion parameters and optimize vehicle maneuverability.

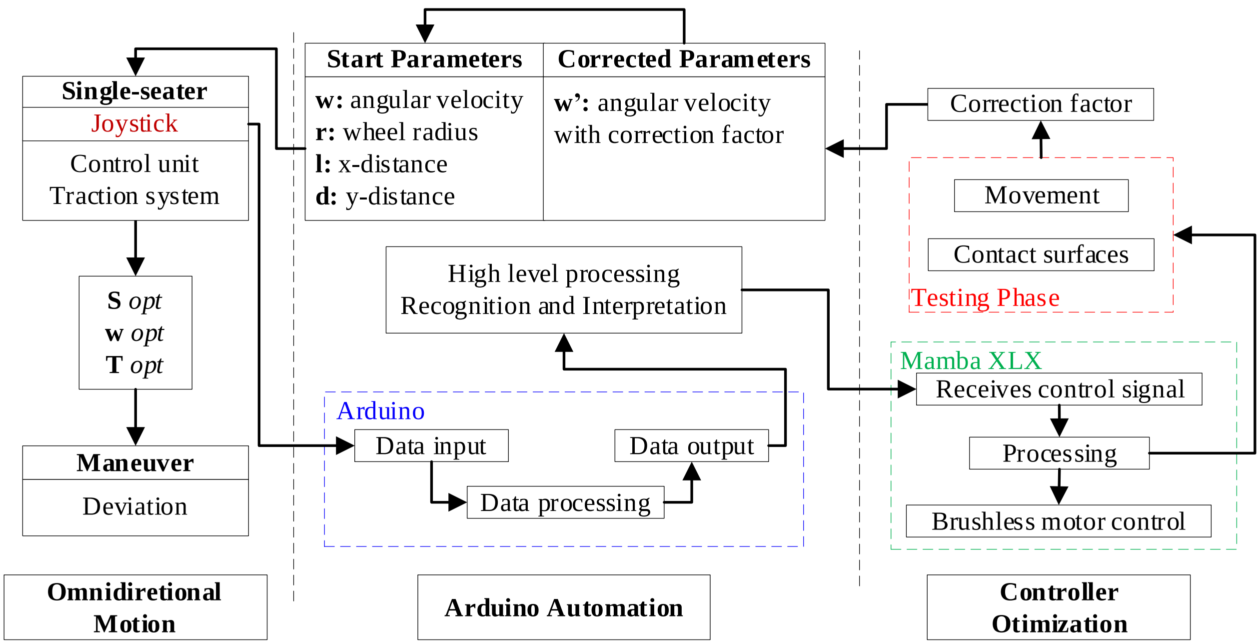

Figure 2: Electronic control scheme

A. Omnidirectional Motion: Design parameters

The control system and component selection were designed with the evaluation of initial parameters, TABLE I.

TABLE I. INITIAL PARAMETERS FOR THE DESIGN OF THE SINGLE-SEATER CONTROL SYSTEM.

Design parameters	Data	Magnitude
Maximum linear velocity (vl)	40	Km/h
Weight to be moved	140	kg
Wheel radius (r)	0.254	m
Single-seater geometry	$l = 0.59$	m
	$d = 0.74$	m

The linear speed *vl* [m/s] required by the single-seater (1) is determined by the ratio of the radius *r* [m] and the rotational speed *w* [rad/s] of each Mecanum wheel provided by the motors. In the test phase *w* will be controlled with a correction factor to obtain the displacement optimization.

$$vl = (\omega * fc) * r \qquad (1)$$

The sum of the electromotive force or torque *T* [Nm] of the motors, allows adequate displacement, and is determined by (2). *I* [A] is the intensity motor current, I_0 is the no-load current, 60/2π is a conversion factor and *Kv* is the motor speed constant in [rpm/V] [12].

$$T = (I - I_0) * \frac{60}{2\pi} * \frac{1}{Kv} \qquad (2)$$

According to the data and equations obtained, the Jeti Phasor Race 2035 series BLDC was selected, which provides an angular velocity of 70000 [RPM]. To achieve the required speed and torque, two gearboxes of 6.75:1 and another of 12:1 were added.

B. Arduino Automation

In Fig.3 the kinematic model is analyzed, detailing the variables that are a function of the geometry of the single-seater.

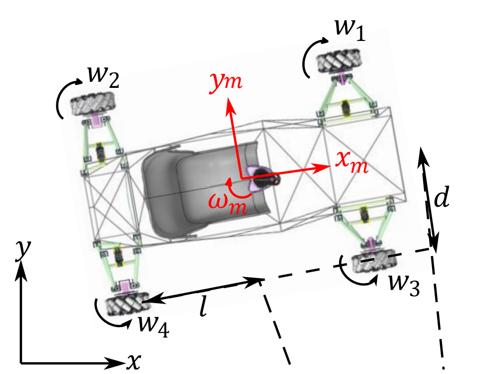

Figure 3: Kinematic Analysis of an Omnidirectional Vehicle.

The joystick works with potentiometers that send signals in ranges from 0 to 1023 in three variables: $eje_{(x,y,z)}$. The values are changed with the function map: *map(value, fromLow, fromHigh, toLow, toHigh)*, so that the MCU performs the kinematic calculation (3) and takes the value of X_m: x-velocity , Y_m: y-velocity, ω_m angular velocity, assigned to the variables $v_{(x,y,w)}$.

$$\begin{bmatrix} w_1 \\ w_2 \\ w_3 \\ w_4 \end{bmatrix} = \begin{bmatrix} 1/r & -1/r & -(l+d)/r \\ 1/r & 1/r & -(l+d)/r \\ 1/r & -1/r & (l+d)/r \\ 1/r & 1/r & (l+d)/r \end{bmatrix} \begin{bmatrix} \dot{x}_m \\ \dot{y}_m \\ \omega_m \end{bmatrix} \qquad (3)$$

The variables $v_{(x,y,w)}$ are sent to a function created with the constants of TABLE I, in order to calculate the angular velocities at each wheel: $w_{(1,2,3,4)}$ [rad/s]. These values are transformed, by using the function: *map(value, fromLow, fromHigh, toLow, toHigh),* into PWM signals that are received by the ESCs. Then, it performs switching sequences on the BLDC inputs to generate the magnetic field required in the operation [13].

The calculation for the maximum commutation frequency F_c [Hz], requires: the maximum revolutions reached RPM_{max}, the number of poles *NP* and the number of phases *PH* of the motor, shown in (4) [13].

$$F_c = \frac{RPM_{max}}{60} \cdot NP \cdot PH \tag{4}$$

In consequence, the ESC has to switch 14000 times per second for proper operation of the BLDC.

C. Controller Optimization:

The control signal modifies the speed and displacement of the single-seater. It is adapted to the test surfaces by implementing a regression model [14] which modifies the PWM signal received by the ESCs for motor control since the automation phase. This model is obtained through (5), in Fig. 4. the data collected in the velocity and displacement tests are presented.

$$\Delta d = (av) + b \tag{5}$$

Δd is the deviation present in the tracking of a trajectory, *a* (6) and *b* (7) are regression coefficients of the analyzed parameters and *v* corresponds to the linear velocity of displacement of the single-seater.

$$a = \frac{S_{\Delta dv}}{S_{v^2}} \tag{6}$$

$$b = \Delta d^{\prime} - av^{\prime} \tag{7}$$

$S_{\Delta dv}$ is the covariance, S_v^2 is the variance, $\Delta d'$ is the mean of the displacement deviation and v' is the mean of the single-seater linear velocity.

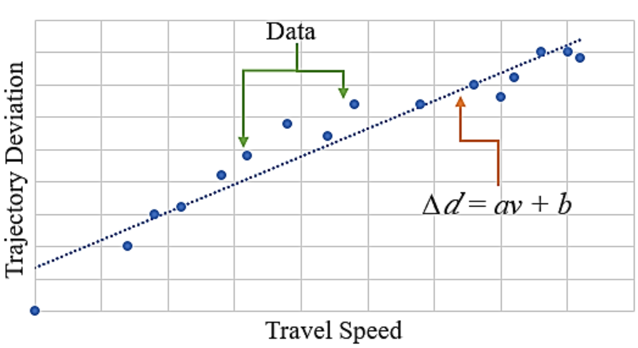

Figure 4: Regression model between the linear velocity of the single-seater and its displacement.

IV. TEST AND RESULTS

In order to control the signal that modifies the rotational speed of the motors, a regression analysis method was implemented. This method determines the relationship between the variation of the linear velocity of the single-seater with the deviation produced during the displacement. The values of the parameters analyzed were obtained by performing a series of tests on two types of surfaces: concrete and asphalt.

A. Concrete Surface.

The first series of tests were performed on concrete with the omnidirectional single-seater moving in the straight-forward, lateral and diagonal directions, under different speeds over a 10 [m] path, the data collected are shown in TABLE II.

TABLE II. TRAJECTORY TESTS ON A FLAT CONCRETE SURFACE

Movement	**Straight**		**Side**		**Diagonal**	
Distance (m)	***Speed (Km/h)***	***Deviation (cm)***	***Speed (Km/h)***	***Deviation (cm)***	***Speed (Km/h)***	***Deviation (cm)***
10	34.15	32	31.5	29	32.6	34
10	26.40	26	26.8	24	25.6	30
10	18.30	19	20.2	19	19.4	27
10	12.60	11	14.5	15	11.6	16
10	6.10	9	5.2	9	5.7	12

B. Asphalt Surface

The second series of tests correspond to the displacement of the omnidirectional single-seater over an asphalt surface in the directions previously mentioned, at different speeds for the 10 [m] distance. The data collected are shown in TABLE III.

TABLE III. TRAJECTORY TESTS ON A FLAT ASPHALT SURFACE

Movement	**Straight**		**Side**		**Diagonal**	
Distance (m)	***Speed (Km/h)***	***Deviation (cm)***	***Speed (Km/h)***	***Deviation (cm)***	***Speed (Km/h)***	***Deviation (cm)***
10	32.60	39	30.7	36	29.6	39
10	24.50	33	22.1	31	23.5	32
10	17.90	25	16.6	20	17.3	27
10	11.47	19	10.5	12	9.4	19
10	5.20	12	6.2	8	5.12	14

With the data obtained on the two surfaces, the regression model, Fig. 4, was determined for the variables studied, where the vertical axis corresponds to the trajectory deviation and the horizontal axis corresponds to the displacement velocity. Through the model the correction factor of 0.9087 is extracted which modifies the displacement velocity, furthermore the model establishes the equation $\Delta d = 0.9087v + 5{,}8385$ which explains the relationship between the two variables. Fig. 5 shows the data dispersion and the deviation as a function of the displacement velocity, which is irregular and not stable on the two surfaces studied.

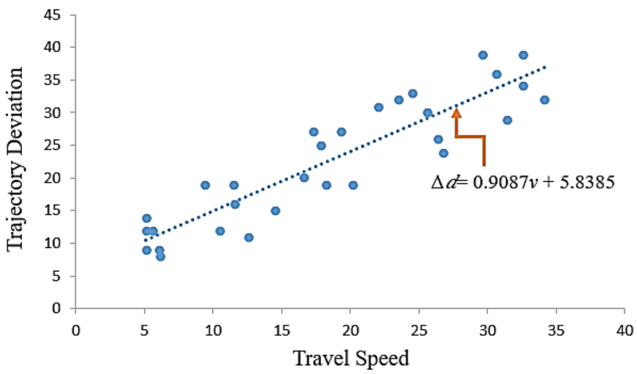

Figure 5: Plot and regression line between the linear velocity of the single-seater and its displacement

The implementation of the correction factor in the automation phase varies the PWM signal and modifies the rotational speed of the motors, thus stabilizing and reducing the deviation in the tracking of a trajectory on both asphalt and concrete surfaces for all the movements that the omnidirectional single-seater is allowed to perform TABLE IV.

TABLE IV. TRAJECTORY TESTS ON A FLAT CONCRETE SURFACE AFTER OPTIMIZATION

Movement	**Straight**		**Side**		**Diagonal**	
Distance (m)	***Speed (Km/h)***	***Deviation (cm)***	***Speed (Km/h)***	***Deviation (cm)***	***Speed (Km/h)***	***Deviation (cm)***
10	32.53	35	29.83	33	30.74	33
10	23.14	30	22.35	29	24.56	29
10	17.56	21	19.04	25	16.2	22
10	10.20	15	11.3	16	9.11	16
10	5.74	9	5.14	10	6.05	11

TABLE V. It shows the results after optimizing the motor control signal for the asphalt surface, in it we can observe a reduction of the deflection in all the movements studied, which represents an improvement in the displacement of the omnidirectional single-seater.

TABLE V. TRAJECTORY TESTS ON A FLAT ASPHALT SURFACE AFTER OPTIMIZATION

Movement	**Straight**		**Side**		**Diagonal**	
Distance (m)	***Speed (m/s)***	***Deviation (cm)***	***Speed (m/s)***	***Deviation (cm)***	***Speed (m/s)***	***Deviation (cm)***
10	34.15	32	31.5	29	32.6	34
10	26.40	26	26.8	24	25.6	30
10	18.30	19	20.2	19	19.4	27
10	12.60	11	14.5	15	11.6	16
10	6.10	9	5.2	9	5.7	12

The data collected after adding the correction factor are presented in Fig 6. There is a reduction in the deviation produced and a smaller dispersion of values compared to the first stage of testing.

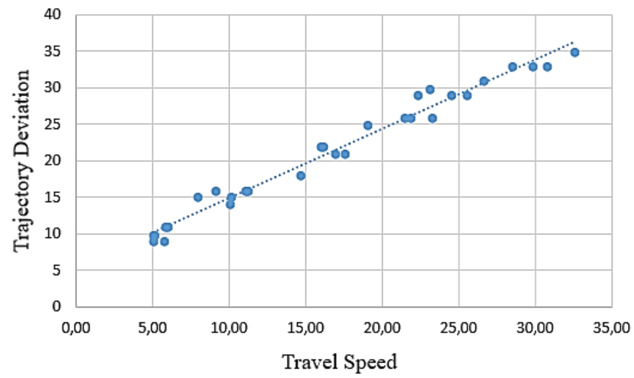

Figure 6: Plot and regression line between the optimized linear velocity of the single-seater and its displacement.

Fig.7 presents the results comparison obtained for the displacement deviation on the two surfaces studied, in the straight-forward, lateral and diagonal directions. It is established that the implemented correction factor, stabilized satisfactorily the velocity and minimized considerably the trajectory deviation.

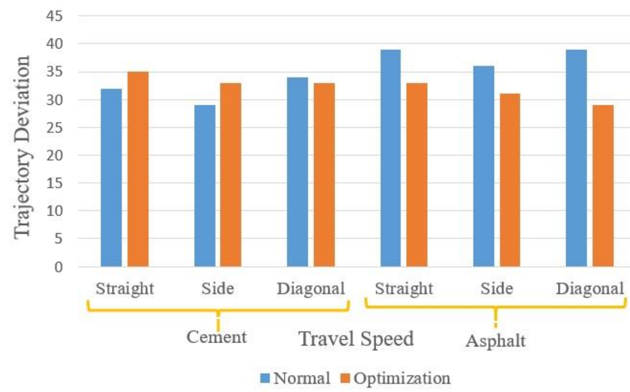

Figure 7: Comparison of results before and after optimization

V. Conclusions

- The control system of the single-seater with omnidirectional traction allows displacement at a maximum measured speed of about 34 [km/h], with small fluctuations caused by the surface conditions and the material of the selected Mecanum wheel. The fluctuations of speed and deviation were reduced after the application of the developed mathematical model. The model relates the two variables studied by regression and predicts the behavior of the vehicle at different speeds.
- It was found that in straight, lateral and diagonal movements, the deviation increases with speed. The mathematical model improved the displacement by 16.66%, making the driving sensation more stable and comfortable for the user.
- The study marks the beginning to reduce the deviation produced in vehicles with Mecanum wheels. Future work is intended to implement a more effective correction method supported by

artificial intelligence and the use of sensors. This will allow predictive assistance to the driver's actions in real time for trajectory following correction.

REFERENCES

[1] T. Shi, F. Zhao, H. Hao, and Z. Liu, “Development Trends of Transmissions for Hybrid Electric Vehicles Using an Optimized Energy Management Strategy,” *Automot. Innov.*, vol. 1, no. 4, pp. 291–299, Nov. 2018, doi: 10.1007/s42154-018-0037-5.

[2] J. A. Sagñay, “Base para inventario de emisiones del parque automotor en la ciudad de Guayaquil,” Aug. 2020, Accessed: Apr. 26, 2021. [Online]. Available: http://www.dspace.espol.edu.ec/handle/123456789/49677

[3] H. Herrera and N. Iván, “Sistema para la toma de decisiones en la congestión vehicular de Quito (Ecuador), mediante análisis de datos sensoriales y sociales,” Jan. 2020, Accessed: Apr. 26, 2021. [Online]. Available: http://dehesa.unex.es/handle/10662/10160

[4] E. Alonso, C. Arpón, M. González, R. Á. Fernández, and M. Nieto, “Economic impact of autonomous vehicles in Spain,” *Eur. Transp. Res. Rev.*, vol. 12, no. 1, p. 59, Oct. 2020, doi: 10.1186/s12544-020-00452-4.

[5] P. Agrawal, S. Sahai, P. Gautam, S. S. Kelkar, and M. R. D, “Designing Variable Ackerman Steering Geometry for Formula Student Race Car,” *Int. J. Anal. Exp. Finite Elem. Anal.*, vol. 8, no. 1, Art. no. 1, Feb. 2021, Accessed: Jul. 20, 2021. [Online]. Available: http://ischolar.info/index.php/ijaefea/article/view/209004

[6] M. F. Vargas, D. S. Sarzosa, and V. H. Andaluz, “Unified Nonlinear Control for Car-like Mobile Robot 4 Wheels Steering,” in *Intelligent Robotics and Applications*, Cham, 2018, pp. 182–194. doi: 10.1007/978-3-319-97589-4_16.

[7] C. Ye, J. Zhang, S. Yu, and G. Ding, “Movement Performance Analysis of Mecanum Wheeled Omnidirectional Mobile Robot,” in *2019 IEEE International Conference on Mechatronics and Automation (ICMA)*, Aug. 2019, pp. 1453–1458. doi: 10.1109/ICMA.2019.8816397.

[8] N. Hacene and B. Mendil, “Motion Analysis and Control of Three-Wheeled Omnidirectional Mobile Robot,” *J. Control Autom. Electr. Syst.*, vol. 30, no. 2, pp. 194–213, Apr. 2019, doi: 10.1007/s40313-019-00439-0.

[9] E. S. Barrionuevo Salazar and B. A. Navas Escudero, “Diseño e implementación de un sistema omnidireccional de transporte para la clasificación y control de calidad usando visión artificial para el Laboratorio de Mecatrónica,” Jul. 2018, Accessed: Apr. 26, 2021. [Online]. Available: http://repositorio.espe.edu.ec/jspui/handle/21000/14708

[10] L. F. Recalde, “Modelación Cinemática y Aplicación de Algoritmos de Control Avanzado en Webots - Modelacion matemática Robot Omnidirecional.” Artil Robotics, Sep. 21, 2020. [Online]. Available: www.artilrobotics.co/cursos

[11] F. A. Aguirre Chuncho and J. E. Ortega Cabrera, “Estudio para la implementación del scooter eléctrico como sistema alternativo de movilidad vehicular en la ciudad de Cuenca,” Jun. 2020, Accessed: Apr. 26, 2021. [Online]. Available: http://dspace.ups.edu.ec/handle/123456789/18708

[12] A. Gong, R. MacNeill, and D. Verstraete, “Performance Testing and Modeling of a Brushless DC Motor, Electronic Speed Controller and Propeller for a Small UAV Application,” in *2018 Joint Propulsion Conference*, American Institute of Aeronautics and Astronautics, 2018. doi: 10.2514/6.2018-4584.

[13] Ł. Przeniosło and M. Hołub, “Efficient electronic speed controller algorithm for multirotor flying vehicles,” in *2018 Innovative Materials and Technologies in Electrical Engineering (i-MITEL)*, Apr. 2018, pp. 1–6. doi: 10.1109/IMITEL.2018.8370482.

[14] S. L. García, A. Arguello, R. Parra, and M. P. Pilay, “Factores que influyen en el pH del agua mediante la aplicación de modelos de regresión lineal,” *INNOVA Res. J.*, vol. 4, no. 2, Art. no. 2, May 2019, doi: 10.33890/innova.v4.n2.2019.909.